



Characterization and impedance study of Ba₂CeZrO₆ double perovskite

Y. Suresh Reddy¹ · Y. Markandeya² · B. Appa Rao¹ · G. Bhikshamaiah¹

Received: 31 August 2017 / Accepted: 7 November 2017 / Published online: 18 November 2017
© Springer Science+Business Media, LLC, part of Springer Nature 2017

Abstract

Double perovskite oxide Ba₂CeZrO₆ is synthesized by sol–gel technique for the first time. The X-ray diffraction pattern at room temperature show that the sample exists in single phase and crystallizes in cubic structure with space group $Fm\bar{3}m$. The lattice parameter is found to be 0.8635 nm. A scanning electron micrograph image of the Ba₂CeZrO₆ sample show uniform distribution of grains size ranging from 2.4 to 3 μm. EDAX spectra showed that Ba₂CeZrO₆ sample contains only Ba, Ce, Zr and O elements which are closer to stoichiometric ratio. Fourier transform infrared spectra of Ba₂CeZrO₆ showed the peaks observed corresponds to CeO₆ and ZrO₆ octahedra indicates the formation of double perovskite structure. The tolerance factor (*t*) of Ba₂CeZrO₆ sample is 0.90 suggests unit cell has a small distortion from ideal cubic structure. Frequency (100 Hz–5 MHz) dependent impedance spectroscopy studies were carried out at different temperatures ranging from room temperature to 400 °C. The decrease in impedance (*Z*), relaxation time (*τ*) and grain, grain boundary resistance and increase in conductivity with increase in temperature shows the semiconducting nature of the Ba₂CeZrO₆ sample. Nyquist analysis showed the contribution of grain and grain boundary resistances for the relaxation process in Ba₂CeZrO₆ sample. The relaxation mechanism in the sample is found to be independent of temperature. The activation energy of Ba₂CeZrO₆ sample is found to be 0.38 eV.

1 Introduction

Double-perovskite oxide (DPO) materials have been studied widely due to their varied structure, physical characteristics and technological applications. The basic structure of double perovskite is in the form of A₂BB'O₆, where A is a large size cation compared to B and B'. The octahedral coordinated B-cations are occupied by two kinds of B and B' cations. The ideal double perovskite oxide structure A₂BB'O₆ can be viewed as a regular arrangement of corner-sharing BO₆ and B'O₆ octahedra, alternating along the three directions of the crystal, with the voluminous A cations occupying the voids in between the octahedral [1–3]. DPO is capable of accommodating all most all elements of periodic table at A, B and B' sites, therefore, these materials exhibit different physical and chemical properties such as magneto resistance,

superconducting, optical, catalytic, thermoelectric and magnetic and also used for different applications as electrode and electrolyte material in fuel cells, magnetic memory materials, spintronic devices, filters, resonators, dielectric and piezoelectric in electronic devices and components for solar cells. In view of this DPO materials have become interesting for researchers for the last several decades.

Impedance spectroscopy is a powerful tool to investigate the electrical properties of the materials. To understand the electrical properties an ac signal is applied as an input perturbation and various electrical parameters are determined. Literature show that most of the DPO materials are synthesized from solid state route and very few reports are available on the synthesis of these materials by sol–gel method. Sol–gel is one of the important synthesis method by which smaller particle size and homogeneous components can be obtained at relatively low sintering temperatures compared to traditional solid state technique [4]. A survey of literature shows that no reports are available on Ba₂CeZrO₆ (BCZ) materials except JCPDS [card no. 48-0335] data published in 1997. In view of this, in the present paper the authors present synthesis of double perovskite BCZ material for the first time from sol–gel method, its characterization using various experimental methods and

✉ G. Bhikshamaiah
gbhyd08@gmail.com

¹ Department of Physics, University College of Science, Osmania University, Hyderabad 500 007, India

² Department of Physics, Nizam College, Osmania University, Hyderabad 500 001, India

detailed frequency dependent impedance studies at different temperatures.

2 Experimental procedure

Double perovskite $\text{Ba}_2\text{CeZrO}_6$ sample has been synthesized using sol–gel method. Stoichiometric amounts of AR grade $\text{Ba}(\text{NO}_3)_2$, $(\text{NH}_4)_2[\text{Ce}(\text{NO}_3)_6]$ and $\text{ZrO}(\text{NO}_3)_2 \cdot \text{H}_2\text{O}$ are taken separately. A solution of 100 ml each are prepared using double distilled water. These solutions are well mixed together in a single beaker. Then citric acid is added to the mixed solution in the ratio of citric acid to metal ions 2:1 for binding the metal ions in the compound by chelation reaction. The resulting mixture is acidic in nature. To reduce acidic nature, the pH of the solution is increased to 7 by adding dilute ammonia. Beaker containing the mixture is heated at 80°C for one day to remove excess amount of water. When mixture is reduced to $\frac{1}{4}$ of its initial volume, a gelation reagent ethylene glycol is added to the solution in the ratio of metal ion to Ethylene glycol 1:1.2. Solution is further heated until a black gel is formed. The gel is heated using Bunsen burner at around 250°C to get dried powders. The dried powder is cooled and ground into fine powder. The powder is preheated at 500°C for 6 h, 700°C for 6 h, 900°C for 6 h and 1100°C for 6 h with intermittent grinding. Finally, the powder is pulverized and made into disc shape pellets of thickness of about 1 mm and diameter of 10 mm. These pellets were then sintered at 1200°C for 6 h.

In order to find crystal structure X-ray diffraction data of BCZ sample was collected in the Bragg angle (2θ) region ranging from 20° to 80° using Phillips Analytical PW 1830 diffractometer with a step scanning of 0.02° per minute at room temperature. The Fourier transform infrared (FTIR) spectrum of the sample was recorded between 200 and 4000 cm^{-1} with Bruker Optics using Tensor 27FTIR spectrophotometer following the KBr pellet technique to identify vibrational units in the molecule. The scanning electron micrograph (SEM) along with energy dispersive X-ray spectrum (EDAX) of the samples was obtained using Oxford Scanning Electron Microscope (Model: INCAX-ac7). In order to study impedance characteristics, silver electrodes were placed on both sides of the disc shape pellet with ultra-fine silver paste and were kept at 200°C for 2 h in a furnace to remove moisture if any. Capacitance (C), impedance (Z), loss tangent ($\tan \delta$) and phase angle (θ) measurements of BCZ pellet sample were carried out using Wayne Kerr electronic (Model: 6400P) precision impedance analyzer at room temperature as function of frequency ranging from 100 Hz to 5 MHz. Similar measurements were carried out at different temperatures beginning with 50°C up to 400°C at every 50°C .

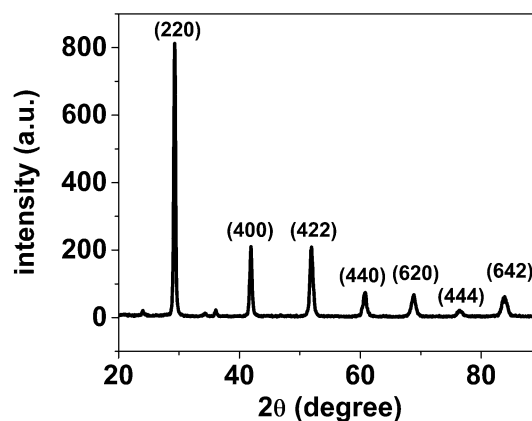


Fig. 1 X-ray diffraction profiles of $\text{Ba}_2\text{CeZrO}_6$ sample recorded at room temperature

Table 1 Comparison of observed and calculated d-values (nm) of X-ray reflection of $\text{Ba}_2\text{CeZrO}_6$ sample at room temperature

2θ ($^\circ$)	hkl	d_{obs} (nm)	d_{cal} (nm)	Difference ($d_{\text{obs}} - d_{\text{cal}}$)	I/I_0
29.32	220	0.304148	0.304256	−0.000108	100
41.87	400	0.215495	0.215425	0.000069	26
51.86	422	0.176077	0.176003	0.000073	25
61.16	440	0.151340	0.152486	−0.001140	14
68.73	620	0.136404	0.136424	−0.000019	8
76.37	444	0.124544	0.124564	−0.000021	2
83.78	642	0.115318	0.115344	−0.000027	7

3 Results and discussion

3.1 Structural characterization

X-ray diffraction profiles of BCZ sample recorded at room temperature is shown in Fig. 1. All the XRD profiles recorded have been indexed and identified as (200), (400), (422), (440), (620), (444) and (642). The observed and calculated values of d-spacing of various profiles are given in Table 1. It can be seen that there is good agreement between experimental and observed d-values indicating the BCZ sample exists in single phase cubic perovskite structure with space group $Fm\bar{3}m$. The lattice parameter of BCZ sample has been evaluated by extrapolating the plot of a_{hkl} vs $\cos\theta \cdot \cot\theta$ as $\theta \rightarrow 0$ and found to be $0.8634\text{ nm} \pm 0.0004$ shown in Fig. 2.

The tolerance factor (t) is a semi quantitative estimates of how close an ABO_3 perovskite to the ideal cubic structure. Higher the deviation of tolerance factor (t) from unity, lesser is the stability of perovskite structure. The tolerance factor for ABO_3 perovskite structure [5] is given by

$$t = \frac{r_A + r_O}{\sqrt{2}(r_B + r_O)} \quad (1)$$

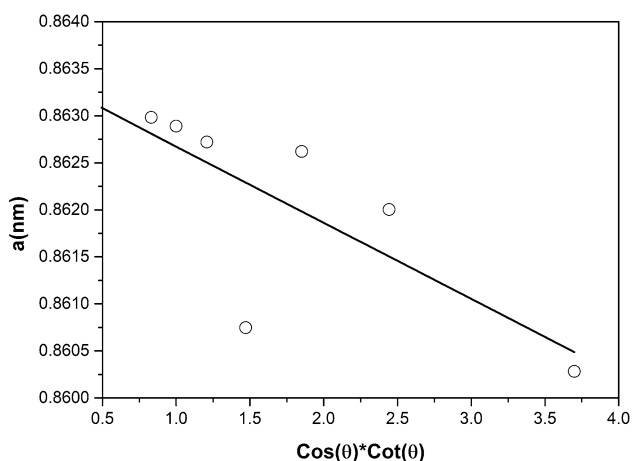


Fig. 2 Lattice parameter (*a*) versus $\text{Cos}(\theta) \text{Cot}(\theta)$ of $\text{Ba}_2\text{CeZrO}_6$ sample at room temperature

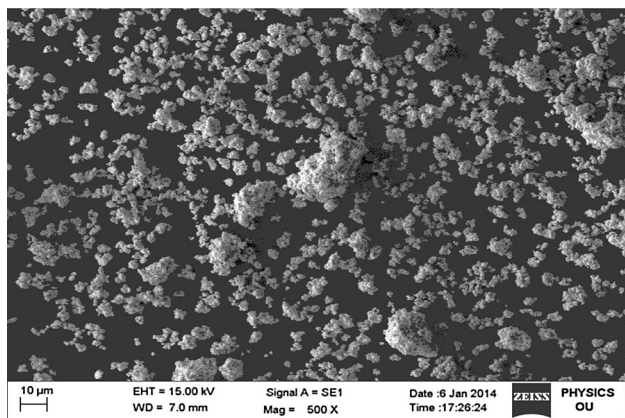


Fig. 3 SEM micrograph of $\text{Ba}_2\text{CeZrO}_6$ sample

where r_A , r_B and r_O are the ionic radii of A, B and Oxygen atoms respectively and $t=1$ corresponds to an ideal cubic perovskite structure. The concept of tolerance factor (t) has been extended to $\text{A}_2\text{BB}'\text{O}_6$ double perovskite [6, 7] and is given as

$$t = \frac{r_A + r_O}{\sqrt{2} \left(\frac{r_B + r_{B'}}{2} + r_O \right)} \quad (2)$$

where r_A , r_B , $r_{B'}$ and r_O are the ionic radii of corresponding ions respectively. In the present study the value of t for BCZ sample has been evaluated using ionic radii of Ba, Ce and Zr and Oxygen atoms and is found to be 0.9035. The value of t suggests that the unit cell of BCZ has a small distortion from ideal perovskite structure.

A SEM micrograph of the BCZ sample is shown in the Fig. 3. It indicates that the sample has a uniform

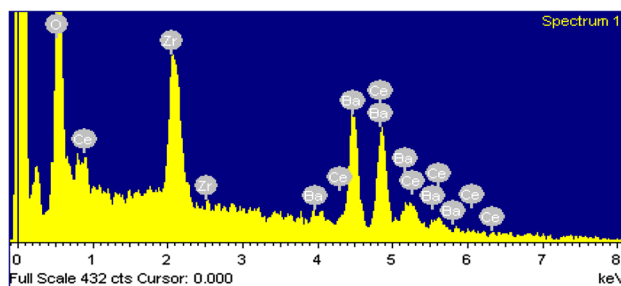


Fig. 4 EDAX spectrum of the $\text{Ba}_2\text{CeZrO}_6$ sample

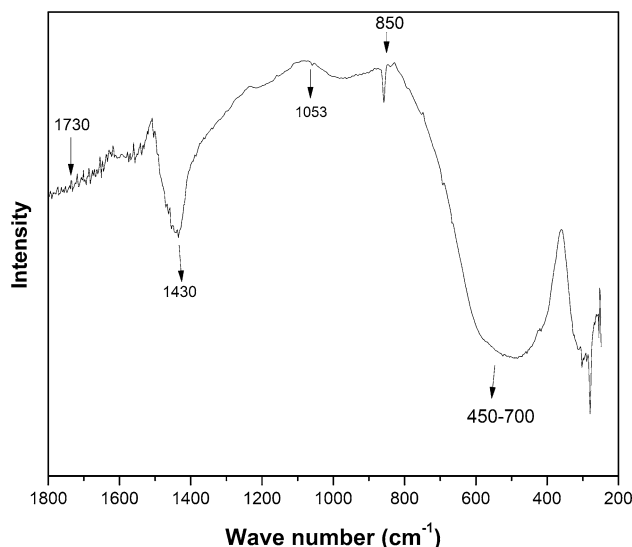


Fig. 5 FTIR spectrum of $\text{Ba}_2\text{CeZrO}_6$ sample

distribution of grains having sizes ranging from 2.4 to 3 μm . The energy dispersive X-ray analysis (EDAX) recorded in the energy range 0–8 keV of the BCZ sample is shown in Fig. 4. It shows well-resolved lines of the constituent atoms Ba, Ce, Zr and O in the sample.

FT-IR spectrum of BCZ sample is shown in the Fig. 5. All the peaks of the spectrum are typical of the material except one small hump at 1730 cm^{-1} [8], which is due to the presence of adsorbed moisture in KBr. The lower energy band in the range 450–700 cm^{-1} is related to the deformational mode of CeO_6 octahedra [8]. The weak band recorded around 850 cm^{-1} can be assigned to IR inactive symmetric stretching vibration of ZrO_6 octahedra due activated by lowering of symmetry [9]. The IR absorption peak found in the present study at 1430 cm^{-1} can be assigned to the CO_2 characteristic vibrations [9]. A small intensity peak at 1053 cm^{-1} likely corresponds to the presence of overtones of the fundamental vibrations in BCZ sample.

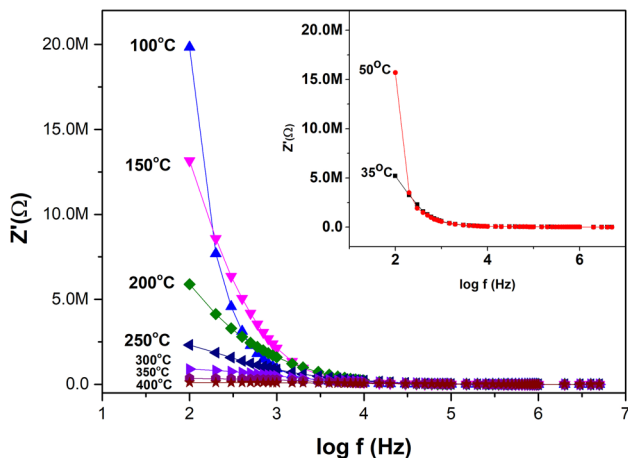


Fig. 6 Plot of Z' versus $\log(f)$ of Ba_2CeZrO_6 at dependence temperatures

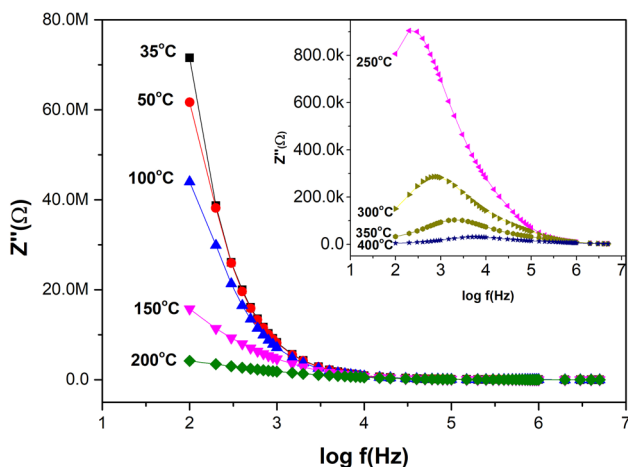


Fig. 7 Plot of Z'' versus $\log(f)$ of Ba_2CeZrO_6 at dependence temperatures

3.2 Impedance study

In order to study the relaxation mechanism of BCZ sample, real part (Z') and imaginary part (Z'') of complex electrical impedance (Z) have been evaluated using impedance (Z) and phase angle (θ). Plots of Z' and Z'' versus $\log(f)$ at various temperatures have been made Figs. 6 and 7 respectively. It

can be observed from Fig. 6 that Z' decreases with increase in frequency at all temperatures indicating the presence of relaxation process in the sample. The magnitude of Z' values at lower frequencies in the temperature range from 100 to 400 °C are found to decrease with increase in temperature indicating reduction of grains and grain boundaries [10]. However, it is found that the value of Z' at low frequency increases with increase in temperatures at 35 and 50 °C as shown in Fig. 6 inset. This may be due to moisture present in the sample. The decrease in Z' with increase in temperature indicates the negative temperature coefficient of resistance (NTCR) showing semiconductor nature of the BCZ sample. This behavior can also found in many other double perovskite oxides [11–14]. It is also found that the value of Z' at higher frequencies merges at all temperatures. This indicates release of space charges that results in the reduction in the barrier properties of BCZ samples at room temperature and can be interpreted by the presence of space charge polarization.

The Z'' plots of BCZ sample in the temperature range 250–400 °C display peaks as shown in Fig. 7 inset. From Figs. 6 and 7 (inset), it can be seen that at lower frequencies Z'' increase while Z' decrease with increase in frequency. The increase in Z'' trend continues up to a peak maximum. The peak maximum values of Z'' are given in Table 2. It can be observed that the peak maximum values of Z'' shifts towards the higher frequency with increase in temperature. This is mainly due to decrease in relaxation time in BCZ sample with increase in temperature. The type and strength of electrical relaxation phenomenon can be described by this behavior in the material. It can be seen that the asymmetric broadening of Z'' peak increases with increase in the temperature. The temperature variation of asymmetric peak broadening in Z'' plot represents the presence of electrical process with a relaxation time distribution as indicated by the peak width. The relaxation species may be due to the presence of electrons at low temperatures and defects at higher temperatures. Impedance data was fitted to Cole–Cole relation given by Eq. (3).

$$Z^* = R_\infty + \frac{(R_0 - R_\infty)}{(1 + j\omega \tau_c)^\alpha} \tag{3}$$

where R_0 and R_∞ are the resistances at very low and very high frequencies, respectively, τ_c is the characteristic

Table 2 Grain and grain boundary resistance and capacitance of complex impedance analysis of Ba_2CeZrO_6 at different temperatures

S. no.	Temp (°C)	Z'' peak frequency (f_c) (Hz)	R_g (Ω)	C_g (F) ($\times 10^{-11}$)	R_{gb} (Ω)	C_{gb} (F) ($\times 10^{-9}$)
1	250	400	150,000	4.5	3,100,000	1.51
2	300	1000	60,000	4.6	990,000	3.25
3	350	1500	21,500	2.1	349,000	2.29
4	400	3000	9000	4.8	101,000	5.85

relaxation time of the system corresponding to the characteristic angular frequency ω at the peak position of Z'' in the Z'' versus $\log(f)$ plot and α is the dimensionless exponent that denotes the angle of tilt of the circular arc from the real axis. The impedance data is fitted with the above equation is shown by solid lines in Fig. 7 for Z'' . The α values have been determined and found to lie between 0.79 and 0.86.

The total resistance of BCZ sample decreases with increase in temperature across entire frequency range showing semiconducting behavior. The values of frequency (f_c) at peak maximum position at different temperatures of Z'' versus $\log f$ plots given in Table 2 found to increase with increase in temperature. In other words, as the temperature increases the most probable relaxation time τ_c ($= 1/2\pi f_c$) decreases. The decrease in relaxation time with increase in temperature as explained in the above para further confirms semiconductor behavior of the BCZ sample. The most probable relaxation time follows the Arrhenius law given by the relation:

$$\tau_c = \tau_0 \exp\left(\frac{E_a}{kT}\right) \tag{4}$$

where τ_0 is the pre-exponential factor, E_a is the activation energy, k is Boltzmann constant and T is absolute temperature. The activation energy E_a calculated from the slope of least-squares fit of the plot drawn between $\log \tau_c$ versus $1000/T$ shown in Fig. 8 and is found to be 0.38 eV.

A plot between scale coordinates of Z'' ($= Z''/Z''_{max}$) and frequency ($\log(f/f_{max})$) is shown in Fig. 9 at different temperatures ranging from 250 to 400 °C in order to see scaling behavior. The figure shows that the entire data of imaginary part (Z'') of impedance collapse into one single curve indicating the relaxation mechanism in BCZ sample is temperature independent, i.e. the scaling nature of Z'' implies

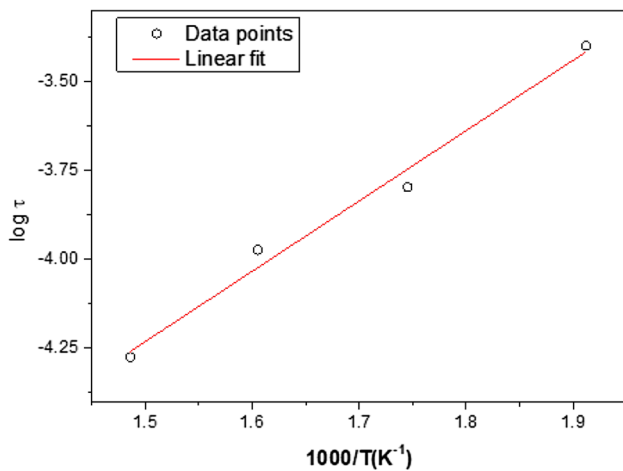


Fig. 8 Plot for $\log \tau$ versus $1000/T$ of Ba_2CeZrO_6 sample

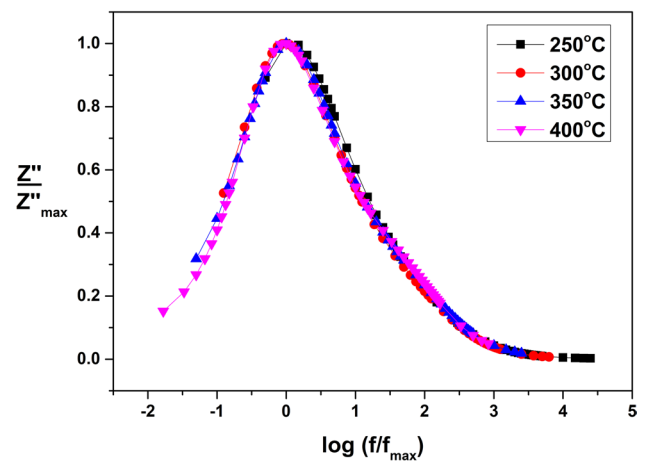


Fig. 9 The scaling behavior of the Z'' of BCZ at temperature 250–400 °C

that the relaxation shows the same mechanism in the entire temperature range in BCZ sample. This behavior is similar to many other DPO materials found in literature [11, 13].

Complex-plane impedance plots (called Nyquist plots, i.e. Z'' vs Z' plot) for BCZ sample at different temperatures are shown in Fig. 10. In the Z -plot, one can expect a separation of the bulk phenomena from the surface phenomena [15–17]. The larger relaxation times of surface polarization compared to that of polarization mechanism in the bulk indicate the respective high capacity phenomenon. This fact usually results in the appearance of two separate area of semicircle in the Z'' versus Z' plots in which one representing the bulk effect at high frequencies while the other represents surface effect in lower frequency range. The values of impedance decreases severely as the temperature increases which shows that the conductivity

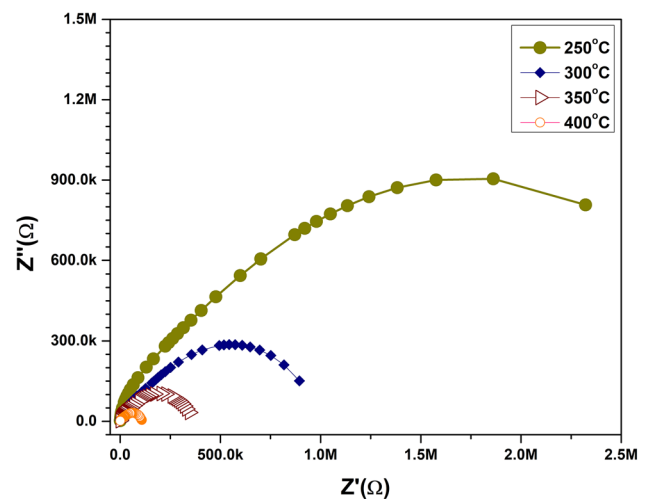


Fig. 10 Complex-plane impedance plots for Ba_2CeZrO_6 at various temperatures

increases sharply with increase in temperature and showing the semiconducting behavior of the material once again.

The analysis of plots of Z'' versus Z' of BCZ sample in the temperature range 250–400 °C show two semicircles. The data has been analyzed for RC equivalent circuit using appropriate software and the value of grain resistance (R_g) and grain boundary resistance (R_{gb}) along with respective capacitances have been evaluated. These values are included in Table 2. As increase of temperature the grain boundaries resistance decreases, indicating the semiconducting behavior of the BCZ sample. It seems that with rise in temperature the grain boundaries effect has assisted in lowering the barrier to the motion of charge carriers laying the way for increased electrical transport. A typical plot of complex plan analysis at 350 °C is shown in Fig. 11. The values of grain and grain-boundary resistances and capacitances can be obtained by an equivalent circuit of two parallel resistance–capacitance (RC) elements connected in series as shown in inset of Fig. 11. Grain and grain boundary effect can be seen in complex plane plot from the two semicircular arcs by the RC elements [10]. The equivalent electrical equations for grain is

$$Z' = \frac{R_g}{1 + (\omega R_g C_g)^2} + \frac{R_{gb}}{1 + (\omega R_{gb} C_{gb})^2} \tag{5}$$

$$Z'' = R_g \left[\frac{\omega R_g C_g}{1 + (\omega R_g C_g)^2} \right] + R_{gb} \left[\frac{\omega R_{gb} C_{gb}}{1 + (\omega R_{gb} C_{gb})^2} \right] \tag{6}$$

where R_g and R_{gb} are the grain and grain boundary resistance and C_g and C_{gb} are the grain and grain boundary capacitances, respectively. We have fitted the experimental data

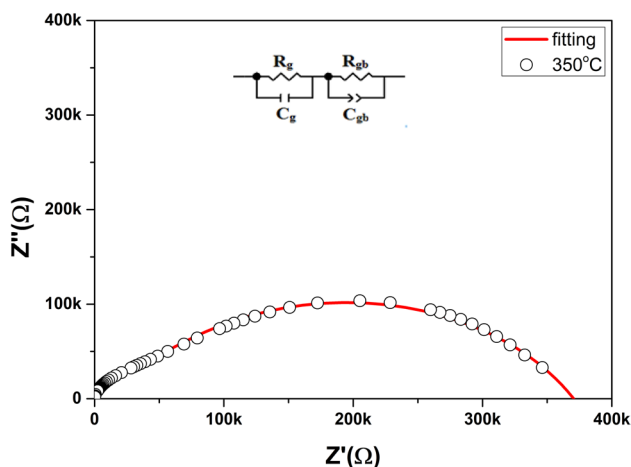


Fig. 11 Complex plane plot of impedance for Ba_2CeZrO_6 at 350 °C (solid line show fitting to the experimental data by RC equivalent circuit)

using these expressions and the best fit of data at 350 °C is shown by solid line in the Fig. 11. The values of grain and grain boundary resistance are found to be decreasing with increase in temperature as shown in Table 2.

3.3 AC conductivity analysis

The admittance(Y) of BCZ sample has been calculated using Z' and Z'' values. Then the values of ac conductivity (σ_{ac}) was computed following the relation $\sigma_{ac} = Y(t/A)$, where t and A are the thickness and area of the pellet respectively. The frequency dependent ac conductivity plots of BCZ sample at various temperatures is shown in Fig. 12. The conductivity shows dispersion that shifts to the higher frequency side with increasing temperature. From Fig. 12, it is clear that σ decreases with decreasing frequency and becomes independent of frequency after a certain value giving dc conductivity (σ_{dc}). The value of σ_{dc} is found to increase with increase of temperature showing the semiconducting behavior.

A plateau region is observed in the lower frequency range where σ_{ac} is frequency independent, this plateau is due to random diffusion of charge carriers at lower frequency. Strong dispersion is observed at higher frequency region for low temperatures. The conductivity spectra follow the Jonscher power law defined as [17]:

$$\sigma = \sigma_{dc} \left[1 + \left(\frac{\omega}{\omega_H} \right)^n \right] \tag{7}$$

where n is dimensionless frequency exponent and ω_H is the hopping frequency of charge carriers. The experimental data is fitted to the above equation with σ_{dc} and ω_H as variables and best fit is shown in the Fig. 12 at various temperatures. The ac conductivity of BCZ sample shows dispersion which

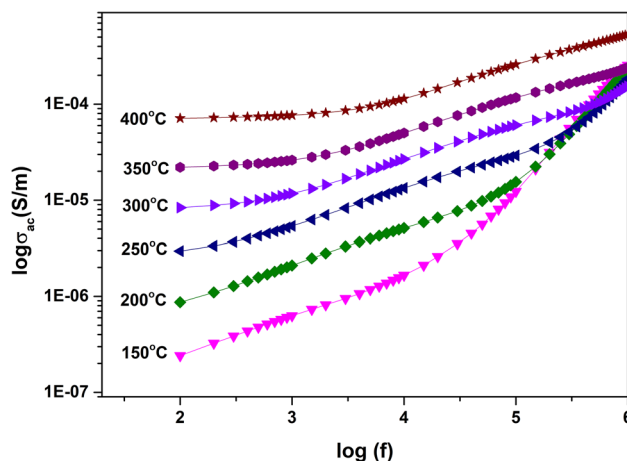


Fig. 12 Variation of ac conductivity with frequency of Ba_2CeZrO_6 sample at different temperatures

shifts to higher frequency side with the increase of temperature revealing the hopping mechanism of conduction.

Arrhenius plot of ac conductivity of BCZ sample at various frequencies is shown in Fig. 13. The activation energies were calculated and tabulated in Table 3. It has been observed that ac conductivity activation energy decreases with frequency.

Reciprocal temperature dependence of dc conductivity is shown in Fig. 14 which obeys Arrhenius law. The activation energy for dc conductivity is found to be 0.37 eV. The value of activation energy suggests that the conductivity in BCZ sample is mainly due to hopping of charge carriers, because the activation energy corresponding to hopping process is small [18, 19].

4 Conclusions

The tolerance factor (t) 0.9035 suggests that the unit cell of $\text{Ba}_2\text{CeZrO}_6$ has a small distortion from ideal cubic structure. The present impedance study suggests semiconducting behavior, presence of grain and grain boundary effect in the relaxation process and relaxation mechanism is temperature independent in BCZ sample. The activation energy of BCZ sample is found to be 0.38 eV.

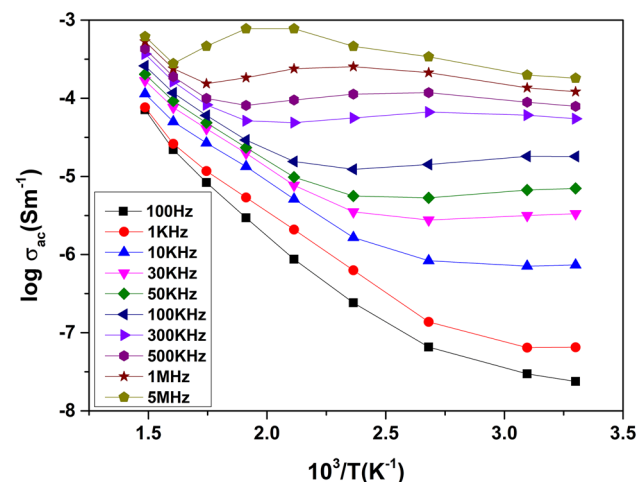


Fig. 13 Reciprocal temperature dependence of ac conductivity for $\text{Ba}_2\text{CeZrO}_6$ sample at different frequencies

Table 3 Activation energies of $\text{Ba}_2\text{CeZrO}_6$ sample at different frequencies

Temperature range (°C)	ac conductivity activation energy (eV)									
	100 (Hz)	1K (Hz)	10K (Hz)	30K (Hz)	50K (Hz)	100K (Hz)	300K (Hz)	500K (Hz)	1M (Hz)	5M (Hz)
100–400	0.378	0.341	0.244	0.182	0.149	0.105	0.055	0.049	0.045	0.043

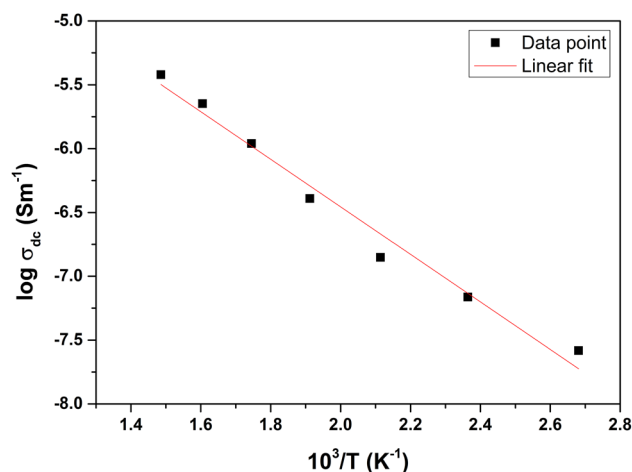


Fig. 14 The temperature dependence of dc conductivity curve for $\text{Ba}_2\text{CeZrO}_6$

Acknowledgements The authors acknowledge Department of Science and Technology, SERB, New Delhi, India for providing financial assistance to carry out this work under the research project (File No. SB/S2/CMP-004/2013). The authors thank the Head, Department of Physics, University College of Science, Osmania University, Hyderabad, India for his encouragement and providing necessary facilities.

References

1. K.I. Kobayashi, T. Kimura, H. Sawada, K. Terakura, Y. Tokura, Room-temperature magnetoresistance in an oxide material with an ordered double-perovskite structure. *Nature* **395**, 677–680 (1998)
2. L. Chen, C. Yuan, J. Xue, J. Wang, B-site ordering and magnetic behaviors in Ni-doped double perovskite $\text{Sr}_2\text{FeMoO}_6$. *J. Phys. D* **38**, 4003–4008 (2005)
3. M. Retuerto, J.A. Alonso, M.J. Martínez-Lope, J.L. Martínez, M. García-Hernández, Record saturation magnetization, Curie temperature, and magnetoresistance in $\text{Sr}_2\text{FeMoO}_6$ double perovskite synthesized by wet chemistry techniques. *Appl. Phys. Lett.* **85**, 266–268 (2004)
4. Y.-Q. Zhai, J. Qiao, Z. Zhang, Magnetic and electrical transport properties of double perovskite $\text{Sr}_2\text{FeMoO}_6$ prepared by sol-gel method. *J. Chem.* **8**(S1), S189–S194 (2011)
5. X.C. Liu, R. Hong, C. Tian, Tolerance factor and the stability-discussion of ABO₃-type ilmenite. *J. Mater. Sci.* **20**(4), 323–327 (2008)
6. C. Bharti, T.P. Sinha, Electrical analysis of a newly synthesized rare earth double perovskite oxide: $\text{Sr}_2\text{CeNbO}_6$. *Physica B* **406**, 624–627 (2011)
7. C. Bharti, T.P. Sinha, Dielectric properties of rare earth double perovskite oxide $\text{Sr}_2\text{CeSbO}_6$. *Solid State Sci.* **12**, 498–502 (2010)

8. C. Bharti, T.P. Sinha, Structural and ac electrical properties of a newly synthesized single phase rare earth double perovskite oxide: $\text{Ba}_2\text{CeNdO}_6$. *Physica B* **406**, 1827–1832 (2011)
9. V. Ratheesh Kumar, P.R.S. Wariar, R. Pazhani, J.K. Thomas, R. Jose, J. Koshy, Development, characterization, sintering, dielectric and optical properties of $\text{NdBa}_2\text{ZrO}_{5.5}$ nanocrystals. *Bull. Mater. Sci.* **35**(7), 1039–1045 (2012)
10. D.K. Mahato, A. Dutta, T.P. Sinha, Impedance spectroscopy analysis of double perovskite $\text{Ho}_2\text{NiTiO}_6$. *J. Mater. Sci.* **45**, 6757–6762 (2010)
11. R. Mukherjee, A. Dutta, T.P. Sinha, Dielectric relaxation of rare earth ordered double perovskite oxide $\text{Ba}_2\text{ErTaO}_6$. *J. Electron. Mater.* **45**(1), 846–852 (2016)
12. C. Bharti, T.P. Sinha, Synthesis, crystal structure, dielectric and optical properties of a new rare earth double perovskite: $\text{Ca}_2\text{CeNbO}_6$. *Physica B* **407**, 84–89 (2012)
13. D.K. Mahato, A. Dutta, T.P. Sinha, Synthesis and electric characterization of rare earth double perovskite $\text{Ho}_2\text{CdZrO}_6$ ceramics. *J. Electroceram.* **29**, 99–105 (2012)
14. Y.Q. Lin, X.M. Chen, X.Q. Liu, Relaxor-like dielectric behavior in $\text{La}_2\text{NiMnO}_6$ double perovskite ceramics. *Solid State Commun.* **149**, 784–787 (2009)
15. K.S. Cole, R.H. Cole, Dispersion and absorption in dielectrics I. Alternating current characteristics. *J. Chem. Phys.* **9**, 341–352 (1941)
16. K.S. Cole, R.H. Cole, Dispersion and absorption in dielectrics II. Direct current characteristics. *J. Chem. Phys.* **10**, 98–105 (1942)
17. M.C.H. Mckubre, J.R. Macdonald, Impedance Spectroscopy, in *Physical Description*, ed. by J.R. Macdonald (Wiley, New York, 1987)
18. D.K. Mahato, A. Dutta, T.P. Sinha, Electrical properties and scaling behavior of rare earth based $\text{Ho}_2\text{CoZrO}_6$ double perovskite ceramics. *Mater. Res. Bull.* **47**, 4226–4232 (2012)
19. A. Dutta, T.P. Sinha, Structural and dielectric properties of $\text{A}(\text{Fe}_{1/2}\text{Ta}_{1/2})\text{O}_3$ [A = Ba, Sr, Ca]. *Mater. Res. Bull.* **46**, 518 (2011)